



OPEN

The disulfidoptosis-related signature predicts prognosis and immune features in glioma patients

Xiong Wang^{1,5}, Jijun Yang^{2,5}, Fengjie Yang³✉ & Ketao Mu⁴✉

Glioma is the most common primary malignant tumor in the central nervous system. Disulfidoptosis is a recently identified programmed cell death in tumor cells overexpressing SLC7A11 under glucose starvation. Clinical prognostic significance of disulfidoptosis has been reported in several tumors, and in this study, we explored the correlation of disulfidoptosis with clinical prognosis, immune cell infiltration, and immunotherapy response in glioma. A total of 1592 glioma patients were included in this study, including 691 glioma patients from The Cancer Genomic Atlas (TCGA), 300 patients with from the Chinese Glioma Genomic Atlas (CGGA) array, 325 patients from CGGA sequencing, and 276 patients from Gene Expression Omnibus (GEO) GSE16011. R software (V4.2.2) and several R packages were applied to develop the risk score model and correlation calculation and visualization. Three disulfidoptosis-related genes, LRPPRC, RPN1, and GYS1, were screened out and applied to establish the risk score model. Low-risk patients exhibit favorable prognosis, and the disulfidoptosis-related signature significantly correlated with clinicopathological properties, molecular subtypes, and immunosuppressive microenvironment of glioma patients. We developed a disulfidoptosis-related risk model to predict the prognosis and immune features in glioma patients, and this risk model may be applied as an independent prognostic factor for glioma.

Abbreviations

CNS	Central nervous system
LGG	Lower-grade gliomas
GBM	Glioblastoma
IDH	Isocitrate dehydrogenase
MGMT	O-6-methylguanine-DNA methyltransferase
PCD	Programmed cell death
SLC7A11	Solute Carrier Family 7 Member 11
NADPH	Nicotinamide adenine dinucleotide phosphate hydrogen
TME	Tumor microenvironment
TCGA	The Cancer Genome Atlas
CGGA	Chinese Glioma Genome Atlas
GEO	Gene Expression Omnibus
OS	Overall survival

Glioma is the most common primary malignant tumor in the central nervous system (CNS), accounting for 47.7% of all malignancies in the CNS¹. Glioma is divided into lower-grade gliomas (LGG, WHO grade II and III) and glioblastoma (GBM, WHO grade IV). GBM patients exhibit more unsatisfactory prognosis than LGG patients. The general median survival time of GBM patients was 12 months after surgery and radiotherapy, while the survival time of LGG patients varied from 1 to 15 years². The current therapeutic interventions including surgery, chemo- and radio- therapy, fails to improve the prognosis of glioma patients especially for the GBM patients, indicating the need for early detection and novel intervention for glioma patients³. Previous cancer genetics have revealed several molecular markers in glioma, such as isocitrate dehydrogenase (IDH) mutations,

¹Department of Laboratory Medicine, Tongji Hospital, Tongji Medical College, Huazhong University of Science and Technology, Wuhan, China. ²Department of Dermatology, Tongji Hospital, Tongji Medical College, Huazhong University of Science and Technology, Wuhan, China. ³Department of Pediatrics, Tongji Hospital, Tongji Medical College, Huazhong University of Science and Technology, Wuhan, China. ⁴Department of Radiology, Tongji Hospital, Tongji Medical College, Huazhong University of Science and Technology, Wuhan, China. ⁵These authors contributed equally: Xiong Wang and Jijun Yang. ✉email: yangfml@126.com; muketao@tjh.tjmu.edu.cn

O-6-methylguanine-DNA methyltransferase (MGMT) promoter methylation, and 1p19q codeletion, and these molecular markers were correlated with favorable prognosis of glioma patients⁴. However, many glioma patients still have minimal responses to these molecular markers targeted therapies, suggesting the need to investigate novel biomarkers for glioma prognosis and treatment prediction.

Programmed cell death (PCD) is induced intentionally accompanied by numerous controlled steps resulting in well-programmed self-destruction during development, including apoptosis, cuproptosis, ferroptosis, pyroptosis, and PANoptosis⁵. Dysregulation of PCD correlates with the development, metastasis, mortality, and recurrence of tumors⁶. Recently, Liu et al. reported a novel metabolic-related PCD, disulfidoptosis, which is induced by excessive accumulation of disulfide in glucose-starved tumor cells overexpressing Solute Carrier Family 7 Member 11 (SLC7A11)⁷. SLC7A11 (also known as xCT) is upregulated in multiple cancers, which imports cystine for glutathione generation and antioxidant defense to block ferroptosis and necroptosis⁸. Under glucose starvation, SLC7A11 overexpression mediated cystine uptake induces nicotinamide adenine dinucleotide phosphate hydrogen (NADPH) depletion, intracellular disulfide accumulation, and ultimate disulfidoptosis⁷. Disulfidoptosis is correlated with prognosis, the tumor microenvironment (TME) and anti-tumor immunity in several tumors, including thyroid carcinoma, bladder cancer, and lung adenocarcinoma⁹⁻¹¹, however, the association between disulfidoptosis and prognosis, TME, and immune therapy response in glioma is unclear.

In the study, we comprehensively explore the role of disulfidoptosis-related genes in the prognosis, TME landscapes, and immune therapy in glioma. We developed and validated a disulfidoptosis-related prognostic model with good performance in predicting prognosis and response to immunotherapy across four independent cohorts.

Materials and methods

Data collection

The Cancer Genome Atlas (TCGA) LGG and GBM datasets were downloaded using the TCGAbiolinks (v2.26.0)¹². The Chinese Glioma Genome Atlas (CGGA) (mRNAseq_325) and CGGA_array datasets (mRNAarray_301) were downloaded from CGGA website (<http://www.cgga.org.cn>)¹³⁻¹⁷. The expression data of GSE16011 was downloaded from the Gene Expression Omnibus (GEO) database (<https://www.ncbi.nlm.nih.gov/geo/query/acc.cgi?acc=GSE16011>), and the clinical data was downloaded from the supplementary data of their published work¹⁸. These data were cleaned and combined using the tinyarray (v2.2.9) R package.

Immunofluorescence staining

The subcellular distribution of these three genes in glioma cell line U-251MG were analyzed using immunofluorescence staining data from HPA database (<http://www.proteinatlas.org>), and the results showed that LRPPRC, RPN1, and GYS1 were in mitochondria, cytosol, and microtubules, respectively.

Disulfidoptosis-related risk signature construction and validation

A total of ten disulfidoptosis-related genes were selected from previous studies, including GYS1, OXSM, NDUFS1, LRPPRC, NDUFA11, NUBPL, NCKAP1, RPN1, SLC3A2 and SLC7A11⁷. Univariate Cox regression and Kaplan–Meier (KM) analyses were performed with survival (v3.5-3) R package to screen disulfidoptosis-related genes significantly correlated with the overall survival (OS). Genes with p values < 0.05 in both analyses were selected for multivariate Cox regression analysis, and TCGA dataset was used as the training cohort. The results of multivariate Cox regression analysis and the KM plots were shown using the survminer (v0.4.9) R package.

Time dependent receiver operating characteristic (ROC) analysis

Time dependent receiver operating characteristic (ROC) curves were calculated using the timeROC (v.0.4) R package to predict the 1-year, 3-year, and 5-year outcomes of glioma patients.

Functional enrichment analysis

The significantly different Kyoto Encyclopedia of Genes and Genomes (KEGG) pathways and Gene Ontology (GO) biological processes between high-risk and low-risk glioma patients were analyzed using the GSVA (v1.46.0) R package¹⁹, and the heatmap was shown with heatmap (v1.0.12) R package.

Evaluation of immune cell fractions

Molecular marker genes of 28 types of immune cells were extracted from previous published work²⁰. The immune cell composition was calculated using the ssgsea method of the GSVA (v1.46.0) R package.

Immune subtype analysis

Tumor samples could be divided into six subtypes: C1 (Wound Healing), C2 (IFN- γ Dominant), C3 (Inflammatory), C4 (Lymphocyte Depleted), C5 (Immunologically Quiet), and C6 (TGF- β Dominant)²⁰. The immune subtype analysis was performed using the ImmuneSubtypeClassifier (v0.1.0) R package.

Figure and plot generation

The venn plot was drawn by tinyarray (v2.2.9) R package. The forest plot and survival KM plot were drawn by survminer (v0.4.9) R package. The timeROC curve was drawn by ggplot2 (v3.4.3) R package. The beeswarm plot was drawn by ggbeeswarm (v0.7.2) R package. The box plot and scatter plot were drawn by ggpunr (v0.6.0) R package.

Results

Construction of risk model using three disulfidoptosis-related genes

A total of ten disulfidoptosis-related genes were selected from previous studies, including GYS1, OXSM, NDUFS1, LRPPRC, NDUFA11, NUBPL, NCKAP1, RPN1, SLC3A2 and SLC7A11⁷. Both univariable Cox regression and KM survival analyses were performed to screen disulfidoptosis-related genes significantly correlated to the prognosis of glioma in all four datasets. A total of three significantly correlated disulfidoptosis-related genes were identified, including LRPPRC, RPN1, and GYS1 (Fig. 1A, Tables S1, 2). The AIC method of Cox Proportional Hazards Model was used to construct the risk model (Fig. 1B, Table 1). The subcellular distribution of these three genes in glioma cell line U-251MG were analyzed using immunofluorescence staining data from HPA database (<http://www.proteinatlas.org>), and the results showed that LRPPRC, RPN1, and GYS1 were in mitochondria, cytosol, and microtubules, respectively (Fig. 1C). We explored their expression in dataset from TCGA and found that LRPPRC was downregulated, while RPN1 and GYS1 were upregulated in TCGA glioma dataset (Fig. 1D). Furthermore, the KM survival plots showed that high expression of LRPPRC was positively correlated with good prognosis, while high expression of RPN1 and GYS1 was positively correlated with poor prognosis (Fig. 1E).

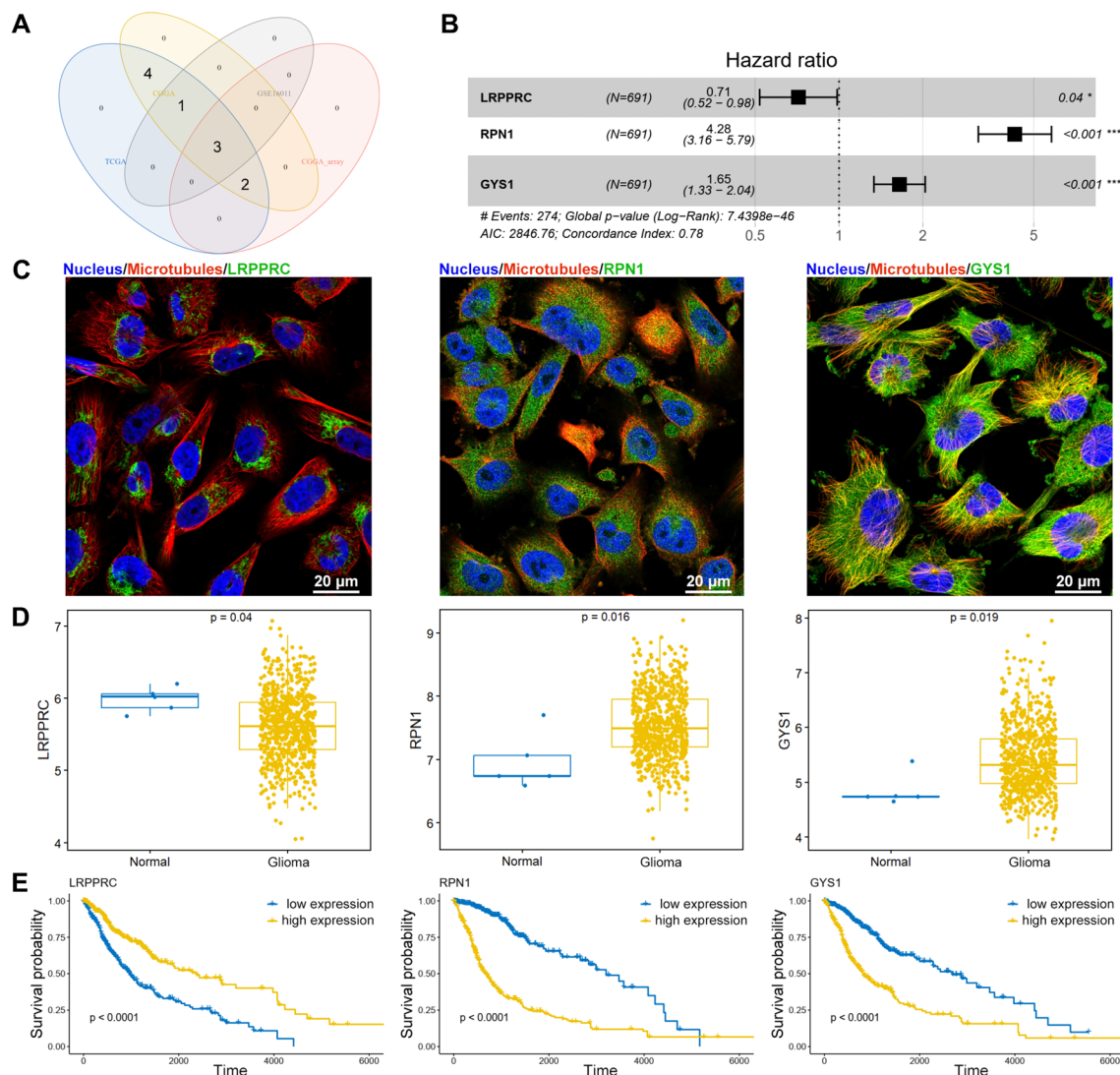


Figure 1. Construction of risk model using three disulfidoptosis-related genes. (A) Intersected genes correlated with prognosis of glioma in both univariable Cox regression and KM survival analyses from the TCGA, CGGA, CGGA-array, and GSE16011 datasets. (B) The Cox Proportional Hazards Model was used to construct the risk model using LRPPRC, RPN1, and GYS1 genes. (C) Immunofluorescence staining of LRPPRC (antibody: HPA036409), RPN1 (antibody: HPA051520), and GYS1 (antibody: HPA041598) in U-251MG glioma cells from HPA database. (D) The expression levels of LRPPRC, RPN1, and GYS1 between glioma (LGG + GBM) and normal control from TCGA were compared and displayed using boxplot. LRPPRC was decreased in glioma, while RPN1 and GYS1 were increased in glioma tissues. (E) K-M survival curves for LRPPRC, RPN1, and GYS1 genes showed that high expression of LRPPRC had better OS, while high expression of RPN1 and GYS1 had worse OS.

Gene	coef	exp(coef)	se(coef)	z	p value
LRPPRC	-0.3358	0.7148	0.1634	-2.055	0.0398
RPN1	1.4536	4.2785	0.1543	9.422	<2e-16
GYS1	0.5002	1.6491	0.1081	4.627	3.71e-06

Table 1. The Cox Proportional Hazards Model using three disulfidoptosis-related genes.

These data suggest that these three disulfidoptosis-related genes were dysregulated in glioma and were associated with the prognosis of glioma.

Evaluation of the disulfidoptosis-related risk signature

The TCGA glioma dataset was used to construct the risk model, and the risk score was calculated using the following formula: risk score = $(-0.3358 \times \text{LRPPRC expression}) + (1.4536 \times \text{RPN1 expression}) + (0.5002 \times \text{GYS1 expression})$. The prognostic prediction potential of the disulfidoptosis-related risk signature was examined with time-dependent ROC curves. The results showed that this risk signature had better AUC values in 3- and 5-year OS prediction and the CGGA dataset had the best prediction potential with an AUC value of 0.85 for 5-year OS (Fig. 2A). Patients were grouped into high and low-risk groups using the cutoff of median risk score value, and the KM survival plots showed that patients with low-risk had better OS in all four datasets (Fig. 2B). The risk score distribution and outcome of patients showed that most alive patients were in the low-risk group, while most dead patients had higher risk scores (Fig. 2C), suggesting the accurate prediction potential of the disulfidoptosis-related risk signature for glioma patients.

Correlation between the disulfidoptosis-related signature and clinicopathological features

Since the disulfidoptosis-related signature showed remarkable correlation with OS of glioma patients and harbored accurate prediction potential, we further explored the correlation between the disulfidoptosis-related signature and clinicopathological features considering malignancy grade, IDH mutation, MGMT promoter methylation, and 1p19q codeletion status. The KM survival plots showed that patients with low-risk had better OS of LGG patients in TCGA, CGGA_array, CGGA datasets, while had better OS of GBM patients in GSE16011 dataset (Fig. 3A). In all four datasets, we found that GBM patients, representing higher grade, had higher risk scores than LGG patients (Fig. 3B). In TCGA dataset, we observed that IDH wildtype, MGMT promoter unmethylated, and 1p19q non-codeletion patients had higher risk scores (Fig. 3C), and similar results were found in CGGA dataset (Fig. 3D). These results indicate that the disulfidoptosis-related signature is significantly correlated with clinicopathological features of glioma patients.

Functional annotation of the disulfidoptosis-related signature

We further investigated the functional annotation of the disulfidoptosis-related signature concerning the KEGG pathways and biological processes. The expression of the three disulfidoptosis-related genes, LRPPRC, RPN1, and GYS1, was examined, and the results showed that RPN1 and GYS1 were increased in high-risk group while LRPPRC was decreased in high-risk group in all four datasets (Fig. 4A). The differences of KEGG pathways and biological processes between low and high-risk groups were compared using the GSVA R package. The significantly different KEGG pathways enriched in high-risk glioma patients involved sugar metabolisms, including glycosaminoglycan, glycosphingolipid, amino and nucleotide sugar (Fig. 4B). The biological processes enriched in high-risk glioma patients involved immune responses, including complement activation, mast cell degranulation, and antigen processing and presentation (Fig. 4C). Disulfidoptosis occurred under glucose starvation, and these results suggest that the three disulfidoptosis-related gene may regulate disulfidoptosis through sugar metabolisms.

Correlation between the disulfidoptosis-related signature and immune features

As immune response biological processes were differentially enriched in low and high-risk glioma patients revealed above, we studied the correlation between the disulfidoptosis-related signature and immune features. Anti-cancer immune response consists of several stepwise events named the cancer-immunity cycle, involving several immune cells and molecules. An inhibitory gene list of the cancer-immunity cycle was downloaded TIP—Tracking Tumor Immunophenotype database²¹, and most of these inhibitory genes were upregulated in high-risk group from all four datasets (Fig. 5A). FGL2, IL10, TGFB1, and VEGFA were secreted immunosuppressive molecules in glioma and were consistently upregulated in high-risk group from all four datasets (Fig. 5B). The immune cell infiltration was analyzed between low and high-risk groups, most immune cells were enriched in high-risk groups including both oncogenic and immunosuppressive cells (Fig. 5C). The glioma patients were divided into six immune subtypes. C4 (Lymphocyte Depleted) and C5 (Immunologically Quiet) accounted for the majority, and C4 subtype representing a high M2 response showed higher ratio in high-risk groups (Fig. 5D). These data indicate that high disulfidoptosis-related risk score represents immunosuppressive status in glioma.

Moreover, the expression of immune checkpoints indicates the response of immunotherapy, and we also found that most immune checkpoint genes were upregulated in high-risk groups (Fig. 6A). PD-1 (PDCD1) and PD-L1 (CD274) have been widely used in immune checkpoint inhibitor immunotherapy, and the results showed that both PD-1 and PD-L1 were increased in high-risk groups, furthermore, disulfidoptosis-related risk score was positively correlated with the expression of PD-1 and PD-L1 (Fig. 6B). These results suggest that disulfidoptosis-related risk signature can predict the immune features of glioma.

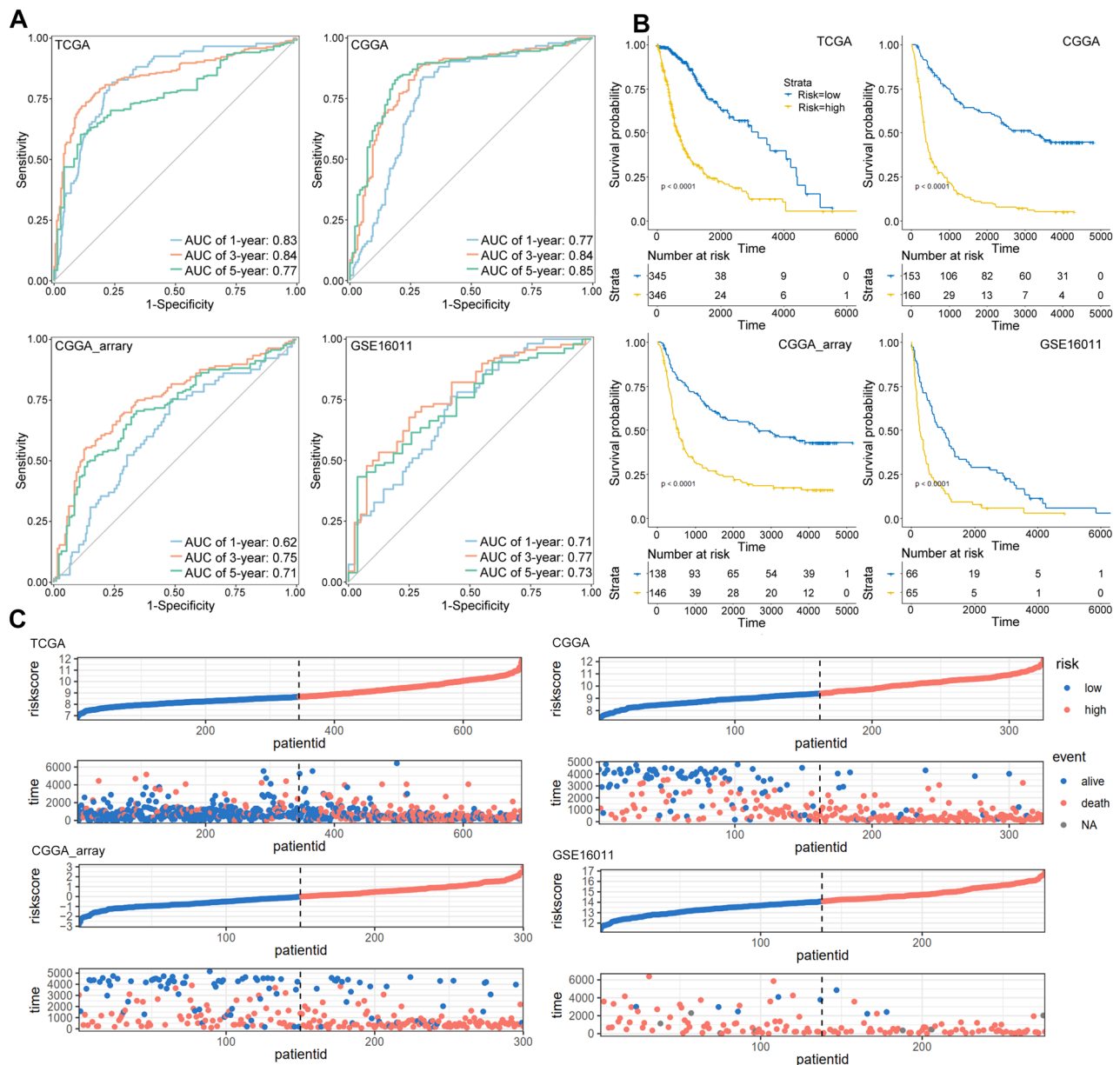


Figure 2. Evaluation of the disulfidoptosis-related risk signature. (A) The 1-, 3-, and 5-year time-dependent OS ROC curves of the disulfidoptosis-related risk signature in the four datasets were calculated using the timeROC R package. (B) The KM survival plots showed that patients with low-risk had better OS. (C) The risk score distribution and outcome of glioma patients in all four datasets.

Discussion

Due to the metabolic imbalance and rapid proliferation, buffering reactive oxygen species (ROS), acidic extracellular pH, hypoxia, and nutrient deprivation to thrive in the tumor microenvironment are the main challenges for cancers. Metabolic reprogramming is an essential hallmark of cancer cells, which results in a high dependence of specific nutrients or metabolites and promotes the survival of cancer cells²². For instance, to mitigating the damaging effects of ROS, cancer cells upregulate the expression of SLC7A11, a cystine-glutamate antiporter, increase the import of cystine to generate cysteine and glutathione. However, under the glucose starvation situation, the cystine accumulates in cancer cells due to the disrupted conversion into cysteine caused by the insufficient supply of NADPH produced from glucose. Eventually, the accumulation of cystine causes aberrant disulfide bonding to the actin cytoskeleton, leading to disulfidoptosis⁷. Liu et al. identified several genes remarkably associated with disulfidoptosis via whole-genome CRISPR-Cas9 screen, including SLC7A11 and its chaperone SLC3A2, and various components of mitochondrial oxidative phosphorylation system (such as NDUFA11, NDUFS1, LRPPRC, and NUBPL)⁷. In this study we comprehensively studied the diagnostic and immunologic potential of these disulfidoptosis-related genes using a risk score model. We established a 3-gene risk model which exhibited good performance in predicting both prognosis and immunotherapeutic response.

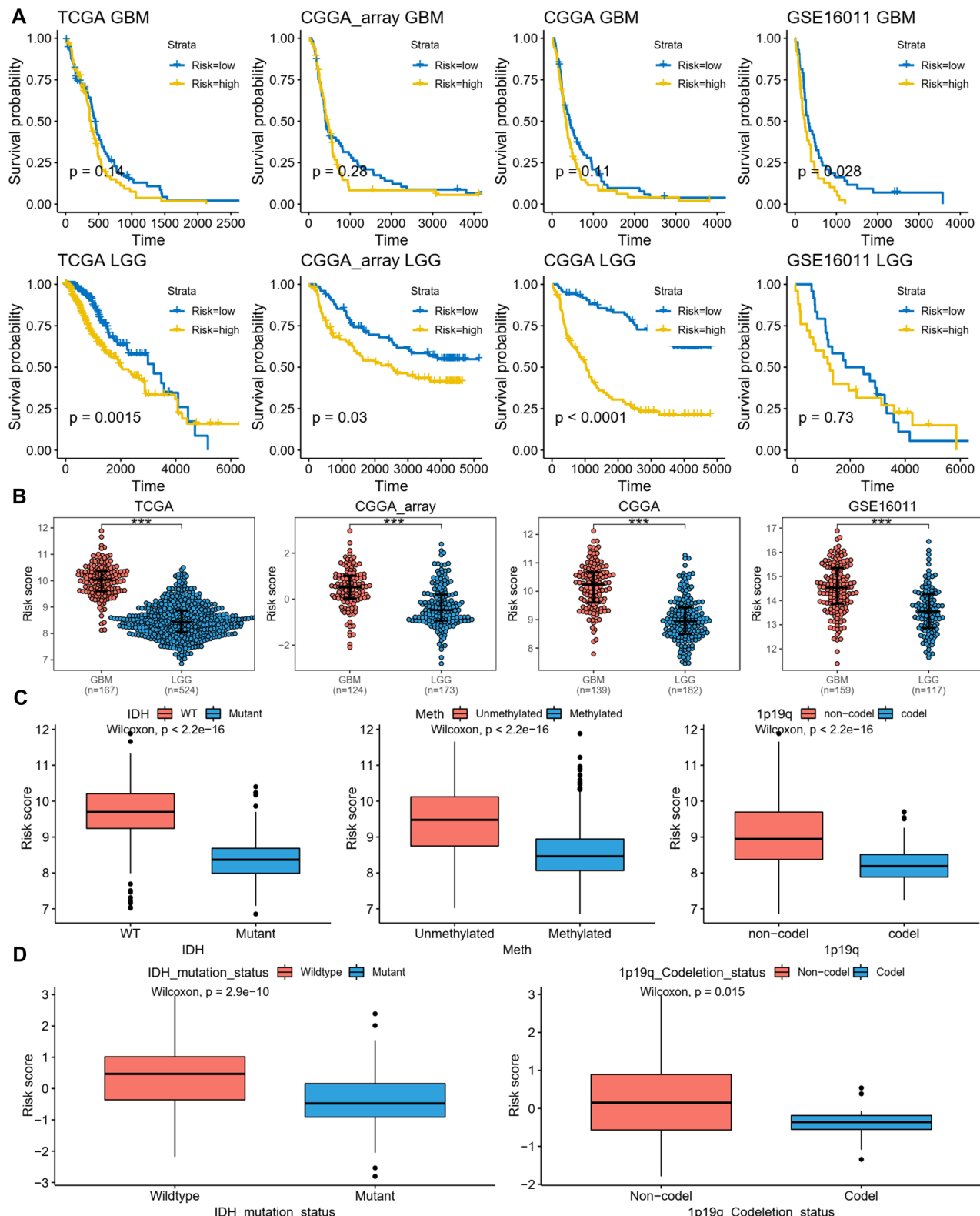


Figure 3. Correlation between the disulfidoptosis-related signature and clinicopathological features. (A) The KM survival plots showed the survival probability of the disulfidoptosis-related signature risk score and OS of GBM and LGG respectively. (B) The beeswarm plot showed the difference of risk scores between GBM and LGG patients in all four datasets. (C) The boxplot showed the difference of risk scores between IDH wildtype (WT) and mutant, MGMT promoter unmethylated and methylated, 1p19q non-codeletion and codeletion patients from TCGA dataset. (D) The boxplot showed the difference of risk scores between IDH wildtype and mutant, 1p19q non-codeletion and codeletion patients from CGGA dataset. *** $p < 0.001$.

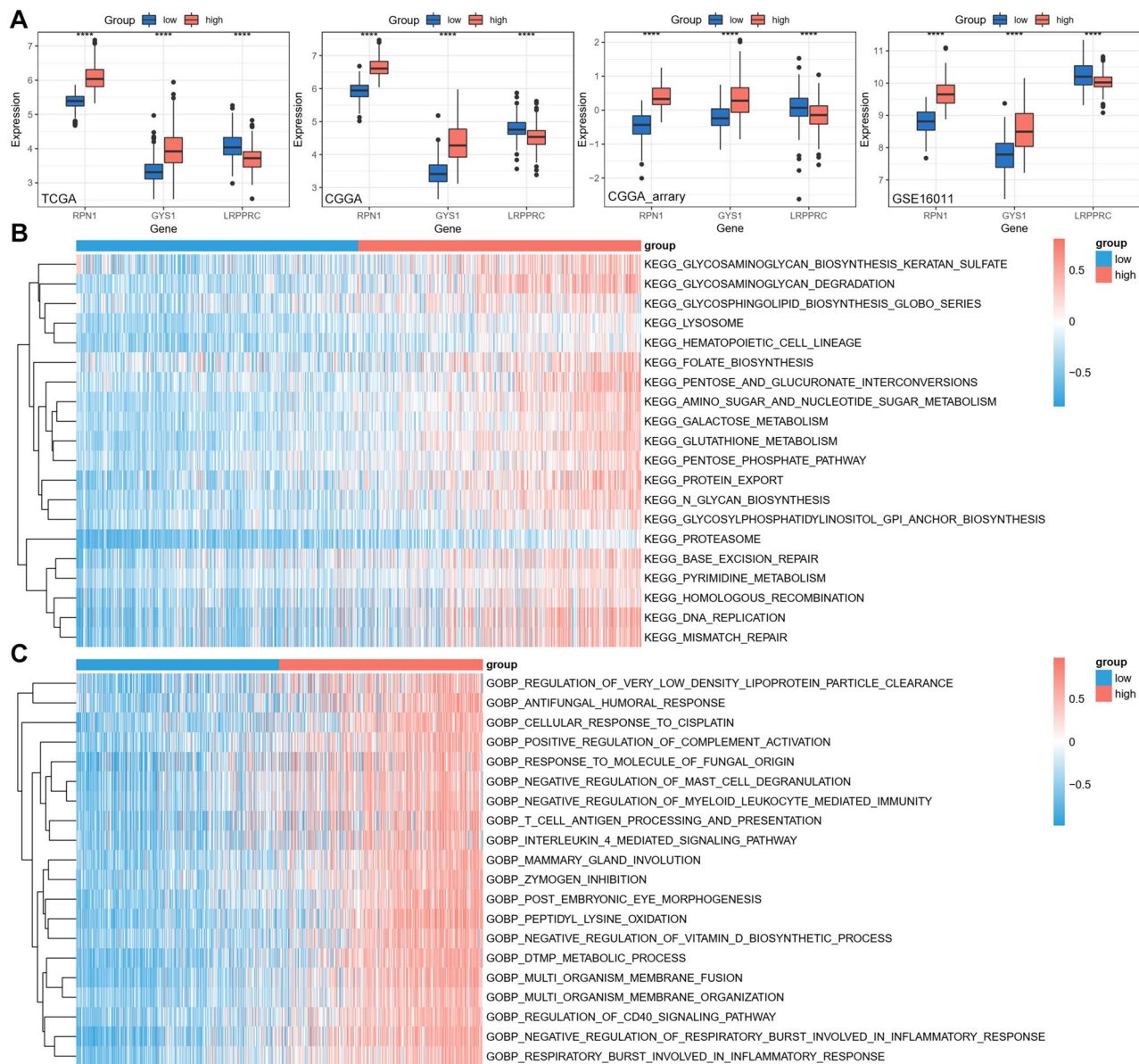


Figure 4. Functional annotation of the disulfidoptosis-related signature. (A) The expression of LRPPRC, RPN1, and GYS1 between low and high-risk glioma patients from all four datasets. (B) The top 20 KEGG pathways enriched in the high-risk glioma patients from TCGA dataset. (C) The top 20 biological processes enriched in the high-risk glioma patients from TCGA dataset. ***p<0.0001.

LRPPRC, RPN1, and GYS1 were identified as survival related disulfidoptosis genes via univariable Cox regression and KM survival analyses among all the four datasets, and a risk score model was constructed using these three disulfidoptosis related genes. LRPPRC is involved in mitochondrial oxidative phosphorylation, RPN1 locates in the endoplasmic reticulum, and GYS1 is a glycogen synthase. Immunofluorescence staining revealed that LRPPRC, RPN1, and GYS1 locate in mitochondria, cytosol, and microtubules, respectively. RPN1 and GYS1 were upregulated in glioma and were negatively correlated with favorable outcome, while LRPPRC1 was downregulated in glioma and positively correlated with favorable outcome. RPN1 encodes a type I integral membrane protein located in endoplasmic reticulum and is involved in the regulation of dolichyl-diphospholigosaccharide-protein glycotransferase activity. Higher RPN1 somatic mutation was found in germline ALK variant glioma patients compared with germline ALK wildtype patients IDH wildtype glioma²³. GYS1 is one of the main regulators of glycogen synthesis, and GYS1 inhibition causes glycogen accumulation in glioblastoma cells, leading to proliferation and migration suppression and formation of ROS, indicating GYS1 inhibition may be a promising therapeutic target for glioma^{24,25}. These studies suggest that the three survival related disulfidoptosis genes may also contribute to the progression of glioma and become the potential therapeutic targets.

Risk score is a convenient and widely used method for the construction of meaningful signatures. Our model was built with disulfidoptosis-related risk scores which showed both accurate prediction of the prognosis of glioma patients and excellent distinction for several glioma molecular subtypes including grade, IDH mutation, MGMT

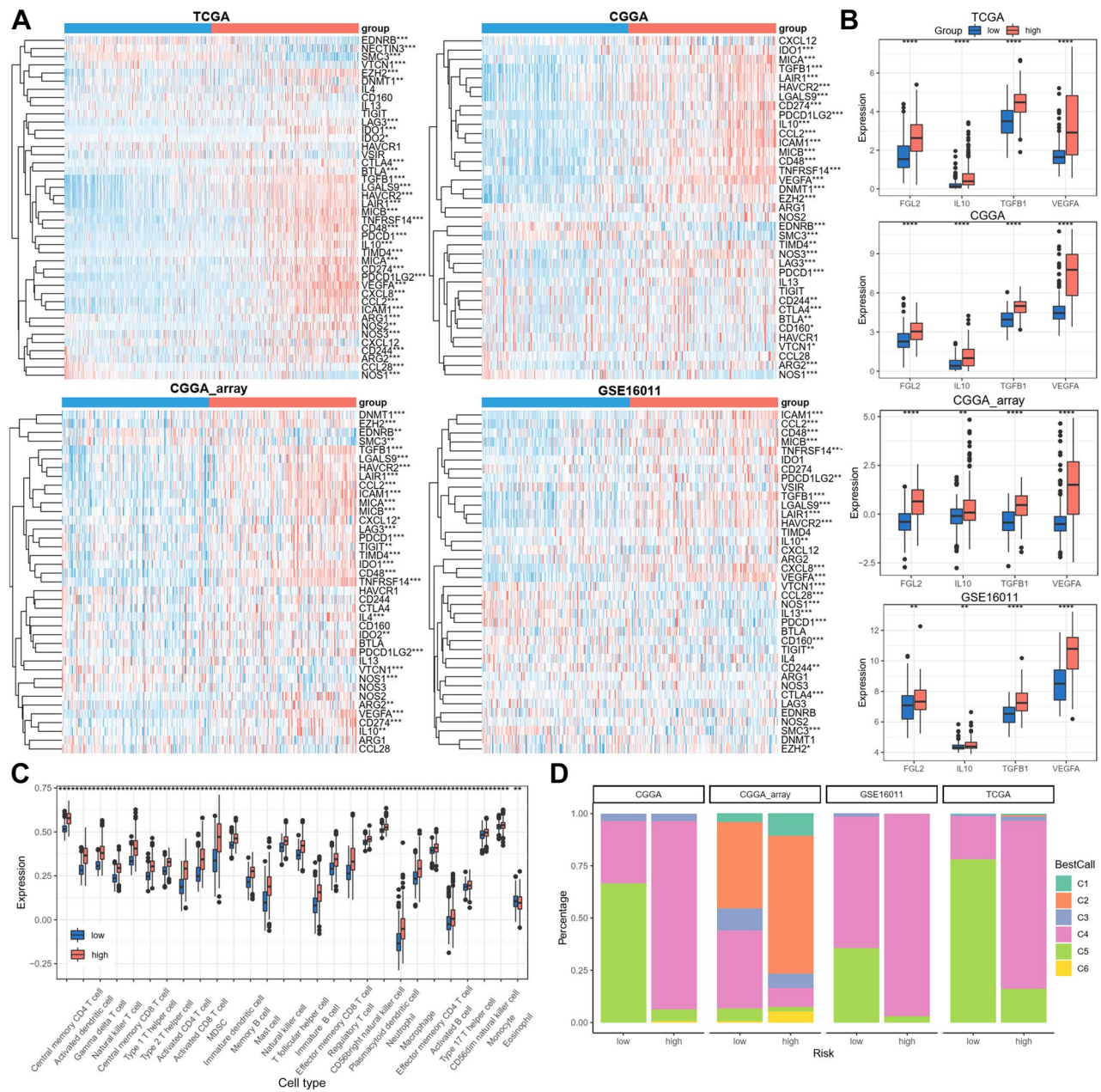


Figure 5. Correlation between the disulfidoptosis-related signature and immune features. **(A)** Expression of the cancer-immunity cycle inhibitory genes between low- and high-risk groups. **(B)** Expression of FGL2, IL10, TGFBI, and VEGFA between low- and high-risk groups. **(C)** Immune cell ratio between low- and high-risk groups from TCGA dataset. **(D)** Distribution of immune subtypes. ** $p < 0.01$, *** $p < 0.0001$.

promoter methylation, and 1p19q codeletion status. The smallest AUC value of 3-year survival was 0.75 found in CGGA_array dataset, indicating good performance for short-term prediction. The AUC values of long-term (5-year) survival prediction were larger than 0.7 with the largest AUC of 0.85 in CGGA dataset. Patients were further divided into high-risk and low-risk subgroups using the median risk score as cutoff value, and low-risk patients showed better prognosis in all four datasets. Moreover, patient distribution also revealed that the alive patients were mainly found in low-risk subgroup, while dead patients were mainly distributed in high-risk subgroup. LGG is low grade glioma (WHO grade II and III), which may progress to the high grade (IV) GBM glioma. Consistently, LGG patients had lower risk scores than GBM patients.

IDH play essential roles in Krebs cycle and cellular homoeostasis via catalyzing the oxidative decarboxylation of isocitrate to generate α -ketoglutarate (α -KG). Cancer genetics revealed that IDH mutation was observed in several malignancies, including acute myeloid leukemia, chondrosarcoma, gliomas, and thyroid carcinoma. The most frequent mutations of IDH such as IDH1^{R132H} mutation exhibits decreased affinity for isocitrate, converting α -KG into D-2-hydroxyglutarate (D-2-HG)²⁶. The accumulation of D-2-HG depletes carbohydrates from the Krebs cycle, leading to metabolic alterations. Moreover, D-2-HG blocks the activity of Ten-eleven translocation methyl cytosine dioxygenase (TET) and histone demethylases lysine-specific demethylase (KDM), resulting in

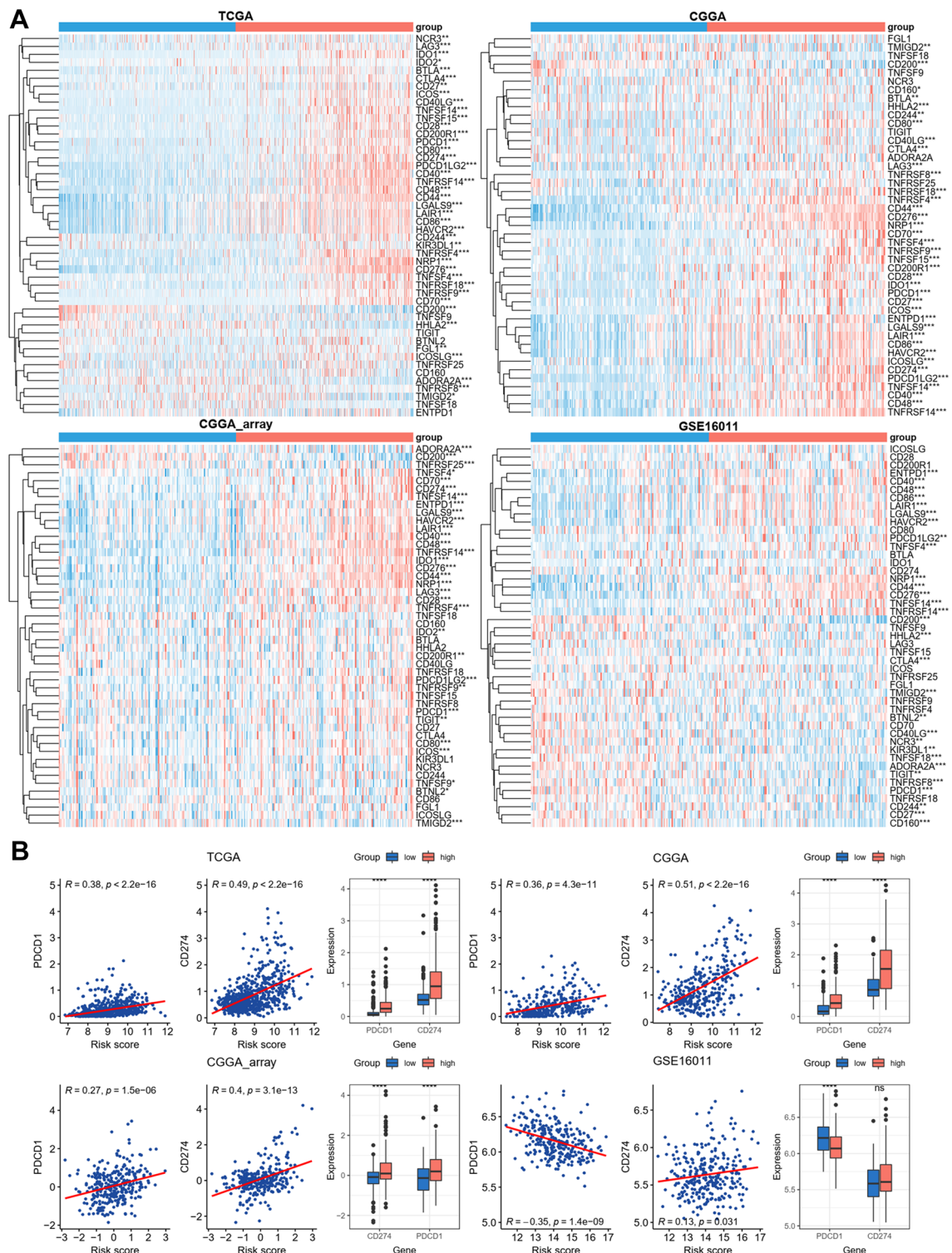


Figure 6. Correlation between the disulfidoptosis-related signature and immune checkpoint genes. **(A)** Expression of immune checkpoint genes between low- and high-risk groups. **(B)** Expression of PD-1 (PDCD1) and PD-L1 (CD274) between low- and high-risk groups. Correlation between disulfidoptosis-related signature risk score and the expression of PD-1 and PD-L1. *** $p < 0.0001$.

CpG island hypermethylation and chromosomal instability²⁷. IDH mutations are primarily detected in grade II and III glioma patients and serves as a favorable prognostic and therapeutic biomarker²⁸. In both TCGA and

CGGA datasets, we found that IDH mutant patients had lower risk scores than the wild type patients, indicating a favorable prognosis.

MGMT promoter methylation, and 1p19q codeletion were other two epigenetic alterations occurred in glioma patients. MGMT promoter methylation is associated with improved OS of GBM patients²⁹. 1p19q codeletion is a combination of loss of the short arm chromosome 1 (1p) and the long arm of chromosome 19 (19q), 1p19q codeletion, MGMT promoter methylation and/or IDH1 mutation signified a better prognosis for glioma patients³⁰. In this study, we found that patients with these molecular aberrations all had lower risk score than the wild type glioma patients. These results suggest that disulfidoptosis-related risk score model is positively correlated with these molecular aberrations and represents a valuable prognostic marker for glioma patients.

We further investigated the affected KEGG pathways and GO terms by differentially expressed genes between high-risk and low-risk glioma patients. Several sugar metabolism pathways and immune response biological processes were significantly enriched in high-risk patients. Disulfidoptosis occurred under glucose starvation, and these results suggest that the three disulfidoptosis-related gene may regulate disulfidoptosis through sugar metabolisms. We also explored the correlation between the disulfidoptosis-related signature and immune features. Several immunosuppressive molecules were consistently upregulated in high-risk group from all four datasets. The immune subtype analysis revealed that the ratio of C4 (Lymphocyte Depleted) subtype, which displays prominent M2 response, was higher in high-risk patients, and C4 immune subtype represents worse prognosis than C5 subtype³¹, further confirming the accuracy of the disulfidoptosis-related risk score model in predicting the prognosis and immune subtypes of glioma patients.

Currently, the immune checkpoint inhibitor therapy has improved patients' survival among several cancers, and becomes one of the most promising cancer therapies³². PD-1 and PD-L1 have been widely used in immune checkpoint inhibitor immunotherapy, and the results showed that both PD-1 and PD-L1 were increased in high-risk groups, and positively correlated with the disulfidoptosis-related risk scores. These results suggest that disulfidoptosis-related risk signature can also predict the immune therapy response of glioma.

In conclusion, we developed a disulfidoptosis-related risk signature using LRPPRC, RPN1, and GYS1 genes. This disulfidoptosis-related risk signature is significantly correlated with prognosis, clinicopathological and immune features, and immune therapy response of glioma patients. The disulfidoptosis-related risk signature may represent an independent prognostic factor for glioma patients.

Data availability

The datasets used during this study can be downloaded from public databases including TCGA, CGGA, and GEO: TCGA-LGG: <https://portal.gdc.cancer.gov/projects/TCGA-LGG>, TCGA-GBM: <https://portal.gdc.cancer.gov/projects/TCGA-GBM>, CGGA (mRNASeq_325): http://www.cgga.org.cn/download?file=download/20220620/CGGA.mRNASeq_325.Read_Counts-genes.20220620.txt.zip&type=mRNASeq_325_counts&time=20220620, CGGA_array (mRNA-array_301): http://www.cgga.org.cn/download?file=download/20200506/CGGA.mRNA_array_301_gene_level.20200506.txt.zip&type=mRNA_array_301_gene_level&time=20200506, GSE16011: <https://www.ncbi.nlm.nih.gov/geo/query/acc.cgi?acc=GSE16011>.

Code availability

The R codes of this study was available at https://github.com/tjhwangxiong/Disulfidoptosis_of_glioma.

Received: 28 June 2023; Accepted: 18 October 2023

Published online: 20 October 2023

References

1. Ostrom, Q. T. *et al.* CBTRUS statistical report: Primary brain and other central nervous system tumors diagnosed in the United States in 2011–2015. *Neuro Oncol.* **20**(suppl_4), iv1–iv86 (2018).
2. Gilbert, M. R. *et al.* A randomized trial of bevacizumab for newly diagnosed glioblastoma. *N. Engl. J. Med.* **370**(8), 699–708 (2014).
3. Wan, R. J., Peng, W., Xia, Q. X., Zhou, H. H. & Mao, X. Y. Ferroptosis-related gene signature predicts prognosis and immunotherapy in glioma. *CNS Neurosci. Ther.* **27**(8), 973–986 (2021).
4. Li, H., Li, J., Cheng, G., Zhang, J. & Li, X. IDH mutation and MGMT promoter methylation are associated with the pseudoprogression and improved prognosis of glioblastoma multiforme patients who have undergone concurrent and adjuvant temozolomide-based chemoradiotherapy. *Clin. Neurol. Neurosurg.* **151**, 31–36 (2016).
5. Vasudevan, S. O., Behl, B. & Rathinam, V. A. Pyroptosis-induced inflammation and tissue damage. *Semin. Immunol.* **69**, 101781 (2023).
6. Lee, S. Y. *et al.* Regulation of tumor progression by programmed necrosis. *Oxid. Med. Cell Longev.* **2018**, 3537471 (2018).
7. Liu, X. *et al.* Actin cytoskeleton vulnerability to disulfide stress mediates disulfidoptosis. *Nat. Cell Biol.* **25**(3), 404–414 (2023).
8. Koppula, P., Zhuang, L. & Gan, B. Cystine transporter SLC7A11/xCT in cancer: Ferroptosis, nutrient dependency, and cancer therapy. *Protein Cell* **12**(8), 599–620 (2021).
9. Chen, H., Yang, W., Li, Y., Ma, L. & Ji, Z. Leveraging a disulfidoptosis-based signature to improve the survival and drug sensitivity of bladder cancer patients. *Front. Immunol.* **14**, 1198878 (2023).
10. Feng, Z. *et al.* Identification a unique disulfidoptosis classification regarding prognosis and immune landscapes in thyroid carcinoma and providing therapeutic strategies. *J. Cancer Res. Clin. Oncol.* **149**, 11157–11170 (2023).
11. Qi, C., Ma, J., Sun, J., Wu, X. & Ding, J. The role of molecular subtypes and immune infiltration characteristics based on disulfidoptosis-associated genes in lung adenocarcinoma. *Aging* **15**(11), 5075–5095 (2023).
12. Colaprico, A. *et al.* TCGAbiolinks: An R/Bioconductor package for integrative analysis of TCGA data. *Nucleic Acids Res.* **44**(8), e71 (2016).
13. Bao, Z. S. *et al.* RNA-seq of 272 gliomas revealed a novel, recurrent PTPRZ1-MET fusion transcript in secondary glioblastomas. *Genome Res.* **24**(11), 1765–1773 (2014).
14. Wang, Y. *et al.* Putamen involvement and survival outcomes in patients with insular low-grade gliomas. *J. Neurosurg.* **126**(6), 1788–1794 (2017).

15. Zhang, K. *et al.* Clinical management and survival outcomes of patients with different molecular subtypes of diffuse gliomas in China (2011–2017): A multicenter retrospective study from CGGA. *Cancer Biol. Med.* **19**(10), 1460–1476 (2022).
16. Zhao, Z. *et al.* Comprehensive RNA-seq transcriptomic profiling in the malignant progression of gliomas. *Sci. Data* **4**, 170024 (2017).
17. Zhao, Z. *et al.* Chinese glioma genome atlas (CGGA): A comprehensive resource with functional genomic data from Chinese glioma patients. *Genomics Proteomics Bioinform.* **19**(1), 1–12 (2021).
18. Gravendeel, L. A. *et al.* Intrinsic gene expression profiles of gliomas are a better predictor of survival than histology. *Cancer Res.* **69**(23), 9065–9072 (2009).
19. Hanzelmann, S., Castelo, R. & Guinney, J. GSVA: Gene set variation analysis for microarray and RNA-seq data. *BMC Bioinform.* **14**, 7 (2013).
20. Charoentong, P. *et al.* Pan-cancer immunogenomic analyses reveal genotype-immunophenotype relationships and predictors of response to checkpoint blockade. *Cell Rep* **18**(1), 248–262 (2017).
21. Xu, L. *et al.* TIP: A web server for resolving tumor immunophenotype profiling. *Cancer Res.* **78**(23), 6575–6580 (2018).
22. Stine, Z. E., Schug, Z. T., Salvino, J. M. & Dang, C. V. Targeting cancer metabolism in the era of precision oncology. *Nat. Rev. Drug Discov.* **21**(2), 141–162 (2022).
23. Bu, L. *et al.* Germline ALK variations are associated with a poor prognosis in glioma and IDH-wildtype glioblastoma. *J. Neurooncol.* **152**(1), 27–36 (2021).
24. Abbadi, S. *et al.* Glucose-6-phosphatase is a key metabolic regulator of glioblastoma invasion. *Mol. Cancer Res.* **12**(11), 1547–1559 (2014).
25. Knudsen, A. M., Boldt, H. B., Jakobsen, E. V. & Kristensen, B. W. The multi-target small-molecule inhibitor SB747651A shows in vitro and in vivo anticancer efficacy in glioblastomas. *Sci. Rep.* **11**(1), 6066 (2021).
26. Dang, L. *et al.* Cancer-associated IDH1 mutations produce 2-hydroxyglutarate. *Nature* **462**(7274), 739–744 (2009).
27. Kohli, R. M. & Zhang, Y. TET enzymes, TDG and the dynamics of DNA demethylation. *Nature* **502**(7472), 472–479 (2013).
28. Yan, H. *et al.* IDH1 and IDH2 mutations in gliomas. *N. Engl. J. Med.* **360**(8), 765–773 (2009).
29. Brandes, A. A. *et al.* MGMT promoter methylation status can predict the incidence and outcome of pseudoprogression after concomitant radiochemotherapy in newly diagnosed glioblastoma patients. *J. Clin. Oncol.* **26**(13), 2192–2197 (2008).
30. Boots-Sprenger, S. H. *et al.* Significance of complete 1p/19q co-deletion, IDH1 mutation and MGMT promoter methylation in gliomas: Use with caution. *Mod. Pathol.* **26**(7), 922–929 (2013).
31. Thorsson, V. *et al.* The immune landscape of cancer. *Immunity* **48**(4), 812–830.e814 (2018).
32. Ghouzlan, A. *et al.* Immune checkpoint inhibitors in human glioma microenvironment. *Front. Immunol.* **12**, 679425 (2021).

Acknowledgements

This study is supported by the National Natural Science Foundation of China (81901713 to KM).

Author contributions

K.M.: research design. J.Y. and F.Y.: data collection. X.W.: data analysis.

Competing interests

The authors declare no competing interests.

Additional information

Supplementary Information The online version contains supplementary material available at <https://doi.org/10.1038/s41598-023-45295-w>.

Correspondence and requests for materials should be addressed to F.Y. or K.M.

Reprints and permissions information is available at www.nature.com/reprints.

Publisher's note Springer Nature remains neutral with regard to jurisdictional claims in published maps and institutional affiliations.



Open Access This article is licensed under a Creative Commons Attribution 4.0 International License, which permits use, sharing, adaptation, distribution and reproduction in any medium or format, as long as you give appropriate credit to the original author(s) and the source, provide a link to the Creative Commons licence, and indicate if changes were made. The images or other third party material in this article are included in the article's Creative Commons licence, unless indicated otherwise in a credit line to the material. If material is not included in the article's Creative Commons licence and your intended use is not permitted by statutory regulation or exceeds the permitted use, you will need to obtain permission directly from the copyright holder. To view a copy of this licence, visit <http://creativecommons.org/licenses/by/4.0/>.

© The Author(s) 2023